

Video Article

# Synthesis of Immunotargeted Magneto-plasmonic Nanoclusters

Chun-Hsien Wu<sup>1,2</sup>, Konstantin Sokolov<sup>1,2</sup>

<sup>1</sup>Department of Biomedical Engineering, University of Texas at Austin

<sup>2</sup>Department of Imaging Physics, University of Texas M.D. Anderson Cancer Center

Correspondence to: Konstantin Sokolov at [ksokolov@mdanderson.org](mailto:ksokolov@mdanderson.org)

URL: <https://www.jove.com/video/52090>

DOI: [doi:10.3791/52090](https://doi.org/10.3791/52090)

Keywords: Chemistry, Issue 90, nanoparticles, plasmonic, magnetic, nanocomposites, magnetic trapping, circulating tumor cells, dark-field imaging

Date Published: 8/22/2014

Citation: Wu, C.H., Sokolov, K. Synthesis of Immunotargeted Magneto-plasmonic Nanoclusters. *J. Vis. Exp.* (90), e52090, doi:10.3791/52090 (2014).

## Abstract

Magnetic and plasmonic properties combined in a single nanoparticle provide a synergy that is advantageous in a number of biomedical applications including contrast enhancement in novel magnetomotive imaging modalities, simultaneous capture and detection of circulating tumor cells (CTCs), and multimodal molecular imaging combined with photothermal therapy of cancer cells. These applications have stimulated significant interest in development of protocols for synthesis of magneto-plasmonic nanoparticles with optical absorbance in the near-infrared (NIR) region and a strong magnetic moment. Here, we present a novel protocol for synthesis of such hybrid nanoparticles that is based on an oil-in-water microemulsion method. The unique feature of the protocol described herein is synthesis of magneto-plasmonic nanoparticles of various sizes from primary blocks which also have magneto-plasmonic characteristics. This approach yields nanoparticles with a high density of magnetic and plasmonic functionalities which are uniformly distributed throughout the nanoparticle volume. The hybrid nanoparticles can be easily functionalized by attaching antibodies through the Fc moiety leaving the Fab portion that is responsible for antigen binding available for targeting.

## Video Link

The video component of this article can be found at <https://www.jove.com/video/52090/>

## Introduction

Hybrid nanoparticles consisting of different materials with distinct physicochemical properties can open new opportunities in biomedical applications including multimodal molecular imaging, therapy delivery and monitoring, new screening and diagnostic assays<sup>1-3</sup>. The combination of plasmonic and magnetic properties in a single nanoparticle is of particular interest because it provides a very strong light scattering and absorption cross-sections associated with plasmon resonances and responsiveness to a magnetic field. For example, magneto-plasmonic nanoparticles were used to increase contrast in dark-field imaging of labeled cells by applying a temporal signal modulation via an external electromagnet<sup>3-5</sup>. More recently, a similar principle was applied in development of a new imaging modality – magneto-photoacoustic imaging, where magneto-plasmonic nanoparticles enable great improvements in contrast and signal-to-background ratio<sup>6,7</sup>. It was also shown that the hybrid nanoparticles can be used for simultaneous capture and detection of circulating tumor cells in whole blood and *in vivo*<sup>8,9</sup>. Furthermore, magneto-plasmonic nanoparticles are promising theranostic agents which can be used for molecular specific optical and MR imaging combined with photothermal therapy of cancer cells<sup>10</sup>.

Several approaches were explored for synthesis of magneto-plasmonic nanoparticles. For example, Yu *et al.* utilized decomposition and oxidation of Fe(CO)<sub>5</sub> on gold nanoparticles to form dumbbell-like bifunctional Au-Fe<sub>3</sub>O<sub>4</sub> nanoparticles<sup>11</sup>. Wang *et al.* have synthesized gold-coated iron oxide nanoparticle by using thermal decomposition method<sup>12</sup>. Some other approaches rely on coating polymer or amine functional molecules onto magnetic core nanoparticles followed by deposition of a gold shell onto the polymer surface to create the hybrid particles<sup>7,13</sup>. In addition, iron-oxide nanoparticles were attached to gold nanorods via electrostatic interactions or a chemical reaction<sup>14,15</sup>. Although these approaches yield magneto-plasmonic nanostructures, they compromise to some extent properties of the magneto-plasmonic combination such as optical absorbance in the near-infrared (NIR) window or a strong magnetic moment both of which are highly desirable in biomedical applications. For example, dumbbell Au-Fe<sub>3</sub>O<sub>4</sub> nanoparticles have a plasmon resonance peak at 520 nm which limits their utility *in vivo* due to high tissue turbidity in this spectral range. Furthermore, the magneto-plasmonic nanoparticles produced by current protocols are limited to just one<sup>11</sup> or few (less than 10)<sup>14,15</sup> superparamagnetic moieties (e.g., iron oxide nanoparticles) that is significantly less than could be achieved in a densely packed nanostructure. For example, a densely packed 60 nm diameter spherical nanoparticle can contain on the order of a thousand of 6 nm superparamagnetic nanoparticles. Therefore, there is a great room for improving magnetic properties of the hybrid nanoparticles. Moreover, some of the previously described protocols are relatively complex and require careful optimization in order to avoid particle aggregation during synthesis<sup>14,15</sup>.

Here, we describe a protocol for synthesis of magneto-plasmonic nanoparticles with a strong magnetic moment and a strong NIR absorbance that addresses major limitations of the current art. The synthesis has its origins in oil-in-water microemulsion method<sup>16</sup>. It is based on assembly of nanoparticles of a desired size from a much smaller primary particles. This approach has been successfully used to produce nanostructures from a single material such as gold, iron oxide, and semiconductor primary particles<sup>16</sup>. We extended it to synthesis of magneto-plasmonic

nanoparticles by, first, making 6 nm diameter gold shell/iron oxide core particles and, then, assembling the primary hybrid particles into the final spherical nanostructure. Assembling primary particles into nanoclusters not only allows enhancing the properties of constituent nanoparticles, such as achieving a stronger magnetic moment while preserving superparamagnetic properties, but also takes advantage of the interactions between individual nanoparticles thus creating new characteristics absent from the constituent nanoparticles, such as strong optical absorbance in the NIR window. This protocol yields hybrid nanoparticles with a high density of magnetic and plasmonic functionalities. After primary particles are synthesized, our method is essentially a simple one-pot reaction. The overall plasmon resonance strength and magnetic moment are determined by a number of primary particles and, therefore, can be easily optimized depending on an application. Furthermore, we also developed a procedure for antibody conjugation to the hybrid nanoparticles for various biomedical applications which require molecular specific targeting. Antibodies are attached through the Fc moiety leaving the Fab portion that is responsible for antigen binding available for targeting.

## Protocol

### 1. Instrumentations and Glassware Preparation

1. Wear appropriate protective equipment, *i.e.*, a lab coat, disposable gloves, and eye protection.
2. Connect a round-bottom flask to a condenser and immerse it in a silicone oil bath with a temperature monitoring by a thermometer. Place a source of heat (*e.g.*, hot plate) under the oil bath (**Figure 1**). Use a thermometer capable of measuring the temperature higher than 260 °C.

### 2. Synthesis of Primary Hybrid Magneto-plasmonic Nanoparticles

1. Making Magnetic Core Nanoparticles
  1. Add 353.2 mg (1 mmol) iron(III) acetylacetonate, 1 ml (2 mmol) oleic acid, 1 ml (2 mmol) oleylamine, 1.292 g (5 mmol) 1,2-hexadecanediol, and 10 ml phenyl ether to a round-bottom flask.
  2. Stir the mixture vigorously using a magnetic stir-bar and heat to 250-260 °C for 1 hr under reflux. Then, wait for the solution to cool down to RT. Ensure the temperature is under 260 °C to prevent boiling of the phenyl ether and prevent a burst of the reaction mixture from the round-bottom flask to the condenser.  
**CAUTION:** The reaction mixture is extremely hot and the chemicals may cause irritation. Must operate under a fume hood and wear appropriate personal protection equipment. Ensure adequate ventilation for the oil bath.  
**NOTE:** The oil bath is kept at 250-260 °C temperature for 1 hr during synthesis of the magnetic nanoparticles. In principle, a Pyrex glass dish can be used for this purpose. However, the maximum continuous temperature for Pyrex glass is ~260 °C according to vendor information. Therefore, a metal container provides a safer option for the reaction as it can withstand a higher temperature and last longer during multiple runs.
2. Deposition a gold shell onto magnetic core nanoparticles
  1. Add 411.5 mg (1.1 mmol) gold acetate, 0.25 ml (0.75 mmol) oleic acid, 1.5 ml (3.0 mmol) oleylamine, 775.3 mg (3 mmol) 1,2-hexadecanediol, and 15 ml phenyl ether to a round-bottom flask.
  2. Add 5 ml suspension of magnetic nanoparticles from step 2.1. Heat the reaction mixture to 180 °C and keep under reflux for 1 hr. Wait for the solution to cool down to RT.
  3. Add 50 ml ethanol to precipitate the hybrid primary nanoparticles followed by centrifugation at  $3,250 \times g$  for 15 min.
  4. Resuspend the precipitate in 25 ml hexane by using a bath sonicator. Add 25 ml ethanol to precipitate the primary hybrid nanoparticles. Centrifuge at  $3,250 \times g$  for 15 min and resuspend the precipitate in hexane. Repeat this step three times.
  5. Dry the precipitated primary hybrid nanoparticles in a vacuum desiccator O/N. Confirm that the particles are completely dry.

### 3. Hybrid Magneto-plasmonic Nanoclusters Synthesis and Size Separation

1. Resuspend 5 mg of dry primary hybrid nanoparticles in 1 ml hexane by using a bath sonicator. Sonicate the nanoparticle suspension until no visible precipitate is present.
2. Add the solution from step 3.1 to 10 ml aqueous solution of sodium dodecyl sulfate (2.8 mg/ml) in a 20 ml glass vial with attached caps. Add the suspension of primary hybrid nanoparticles drop by drop to avoid mixing of the two phases before the next step.
3. Sonicate the two-phase solution in a bath sonicator for 2 hr, followed by heating in a water bath at 80 °C for 10 min. Wait for the solution to cool down to RT.
  1. Fill water to the operating level line of the sonication bath. Center the glass vial in the sonication bath. An emulsion forms immediately between the two phases. Shake the two-phase solution by hand after beginning of the sonication; this facilitates mixing between the phase containing primary hybrid nanoparticles and the bottom aqueous phase.  
**NOTE:** Be aware that the sonicator will heat up after 2 hr of operation.
4. Centrifuge the hybrid nanocluster suspension at  $100 \times g$  for 30 min. Collect both the precipitate and the supernatant. Resuspend the precipitate in 0.1 mM sodium citrate under 10 min sonication. The expected size of the nanoclusters is ~180 nm in diameter.
5. Transfer the supernatant from step 3.3 to a new conical tube.
6. Centrifuge the suspension from step 3.4 at  $400 \times g$  for 30 min. Collect both the precipitate and the supernatant. Resuspend the precipitate in 0.1 mM sodium citrate under 10 min sonication. The expected size of the nanoclusters is ~130 nm in diameter.
7. Transfer the supernatant from step 3.5 to a new conical tube.
8. Centrifuge the suspension from step 3.6 at  $1,500 \times g$  for 30 min. Collect the precipitate and resuspend in 0.1 mM sodium citrate under 10 min sonication. The expected size of the nanoclusters is ~90 nm in diameter.
9. Add 300  $\mu$ l nanocluster suspension to a 96-well microplate reader for measuring a UV-Vis-NIR absorption spectrum. Drop 10  $\mu$ l nanocluster suspension onto carbon-coated copper grid for TEM imaging.

## 4. Conjugation of Monoclonal Antibodies to Nanoclusters

1. Prepare 100  $\mu$ l monoclonal antibody solution (1 mg/ml) in PBS, pH 7.2, e.g., anti-Epidermal Growth Factor Receptor 2 (HER2) antibodies or anti-Epidermal Growth Factor Receptor 1 (EGFR) antibodies.
2. Add the antibody solution from step 4.1 to 3.9 ml 4 mM HEPES, pH 7.2. Centrifuge the solution through a 10 k MWCO centrifugal filter at 3,250 x g for 20 min at 8 °C. Resuspend the antibody in 4 mM HEPES, pH 7.2, to a final volume of 100  $\mu$ l.  
NOTE: This step is carried out to replace the original media in the antibody solution with HEPES.
3. Add 10  $\mu$ l of 100 mM NaIO<sub>4</sub> to 100  $\mu$ l of antibody solution. Cover the reaction vial with an aluminum foil at RT and mix for 30 min using an orbital shaker.
4. Quench the reaction by adding 500  $\mu$ l of 1x PBS.
5. Add 2  $\mu$ l of 46.5 mM linker solution (dithiol aromatic PEG6-CONHNH<sub>2</sub>) to the antibody solution from step 4.4 and shake for 1 hr at RT.
6. Filter the solution using a 10 k MWCO centrifuge filter at 3,250 x g for 20 min at 8 °C. Resuspend the antibody in 1x PBS to a final volume of 100  $\mu$ l which leads to an antibody concentration of ~1 mg/ml.
7. Mix 100  $\mu$ l nanocluster suspension at O.D. ~1.0 with 1  $\mu$ l modified antibodies from step 4.6 (1 mg/ml) for 120 min at RT.
8. Add 10  $\mu$ l of 10<sup>-3</sup> M 5 kDa thiol PEG and shake for 15 min at RT.
9. Centrifuge the solution at 830 x g for 3 min. Discard the supernatant and resuspend the sediment in 100  $\mu$ l 2% w/v 5 kDa PEG in PBS, pH 7.2.
10. Measure the absorbance spectrum of the antibody-conjugated nanoclusters and compare to the absorbance spectrum of the bare nanoclusters. Expect a couple of nanometer red shift after the conjugation.
11. If the nanoparticles aggregate as shown by a significant shift with an increase in O.D. in the red-NIR region, increase the concentration of thiol PEG to 5 x 10<sup>-3</sup> M. Also, increase the incubation time with thiol PEG to 30 min and decrease the centrifugal speed in 200 x g increments.
12. For cancer cell labeling test, add the antibody conjugated nanoparticles from step 4.9 to cancer cell suspension in either medium or 1x PBS (1 ml ~10<sup>6</sup> cells) and mix for 60 min.

## Representative Results

A scheme for synthesis of immunotargeted magneto-plasmonic nanoclusters is shown in **Figure 2**. First, magnetic Fe<sub>3</sub>O<sub>4</sub> iron oxide nanoparticles are synthesized via thermal decomposition method. Then, a thin ca. 1 nm gold shell is deposited on the iron oxide core particles via thermal decomposition. The primary ca. 6 nm hybrid nanoparticles serve as seeds to create magneto-plasmonic nanoclusters by utilizing an oil-in-water microemulsion approach. The nanoclusters are functionalized with monoclonal antibodies for molecular specific targeting.

The size of as-synthesized iron oxide core nanoparticles is ~5 nm in diameter. After gold shell deposition onto the magnetic core, the size of primary iron oxide core/gold shell nanoparticles increases to ~6 nm in diameter. The colloidal color changes from brown for iron oxide nanoparticles to red-purple after deposition of the gold shell and, finally, to purple-gray color after assembly of the primary particles into ~180 nm diameter spherical nanoclusters (**Figure 3**). UV-Vis spectra show that primary iron oxide core/gold shell nanoparticles have a distinctive resonance peak at 530 nm that is not present in bare iron oxide particles (**Figure 4**). Upon cluster formation, the spectrum changes markedly and exhibits a strong broad NIR absorbance (**Figure 4**).

The nanoclusters are conjugated with monoclonal antibodies to specifically target biomolecules of interest. The conjugation protocol utilizes a heterofunctional polyethylene glycol (PEG) linker that attaches Fc region of antibodies to the nanocluster surface. One end of the linker has a hydrazide moiety which interacts with oxidized glycosylated antibody moiety. The other end of the linker contains a di-thiol group which has a strong affinity to the gold surface of the nanoclusters. To demonstrate molecular targeting we have chosen an EGFR positive skin cancer cell line (A-431) and a HER2 positive breast cancer cell line (SK-BR-3). Nanoclusters were functionalized with either anti-EGFR or anti-HER2 antibodies followed by mixing with A-431 or SK-BR-3 cancer cells, respectively. In **Figure 5**, a bright gold-orange color on A-431 and SK-BR-3 cancer cells indicates molecular specific binding of nanoclusters to corresponding receptors on cancer cells. In contrast, untargeted PEGylated nanoclusters did not interact with cancer cells. These results show molecular specificity of the functionalized nanoclusters.



**Figure 1. An experimental setup for synthesis of primary iron oxide core/gold shell nanoparticles.** A round-bottom flask is connected to a condenser. The reaction is carried out in an oil bath under temperature monitoring by a thermometer.

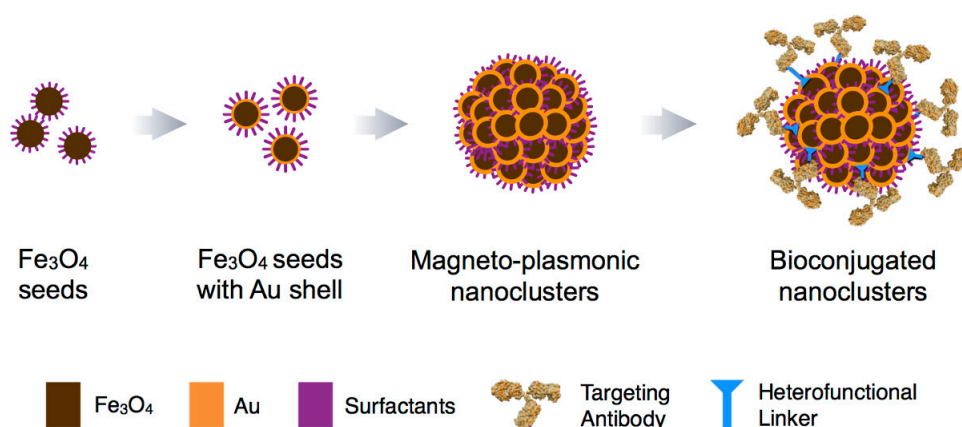


**Figure 2. A schematic illustrating major steps in synthesis of immunotargeted magneto-plasmonic nanoclusters.** [Please click here to view a larger version of this figure.](#)



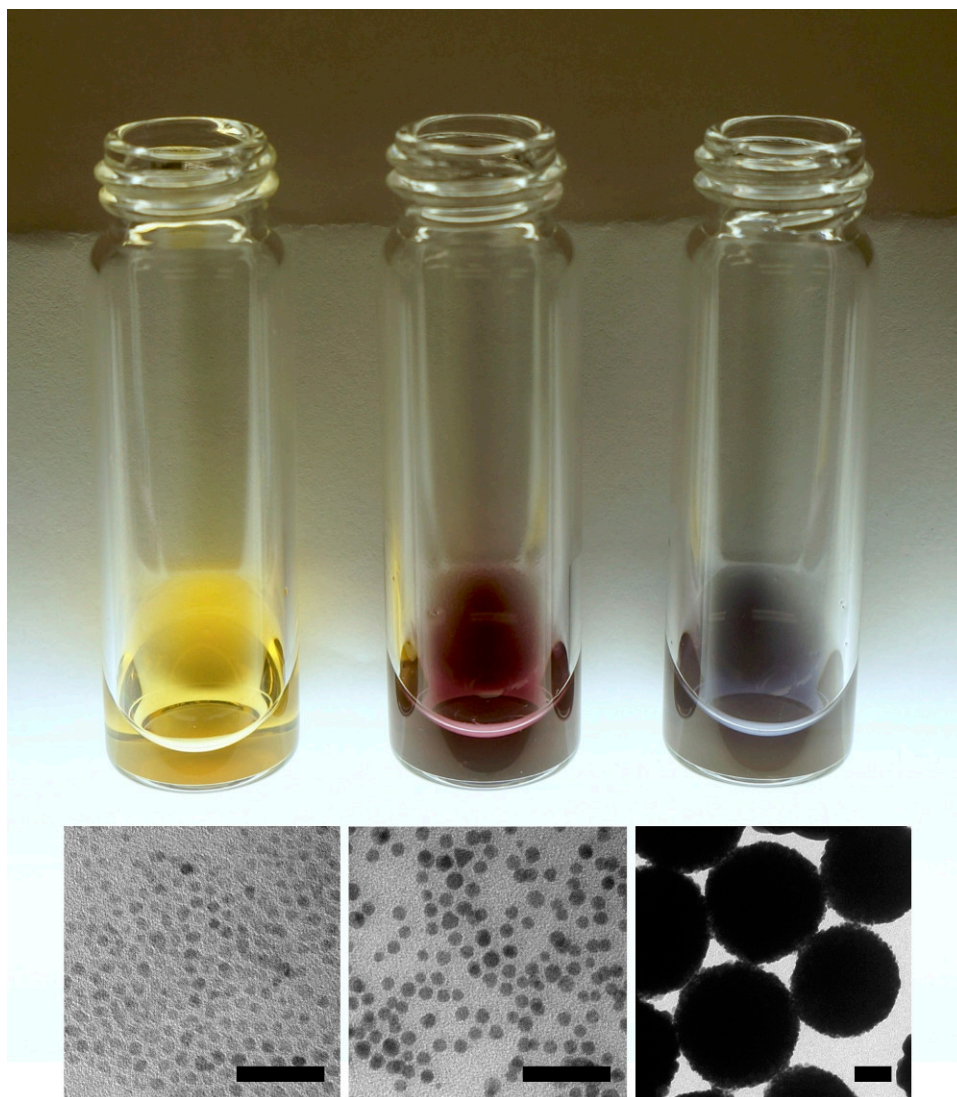


**Figure 3. TEM images and color of colloidal suspensions of nanoparticles:** (Left) iron oxide core nanoparticles; (Middle) gold-coated iron oxide nanoparticles; (Right) hybrid magneto-plasmonic nanoclusters. Scale bar for TEM images is 50 nm. [Please click here to view a larger version of this figure.](#)

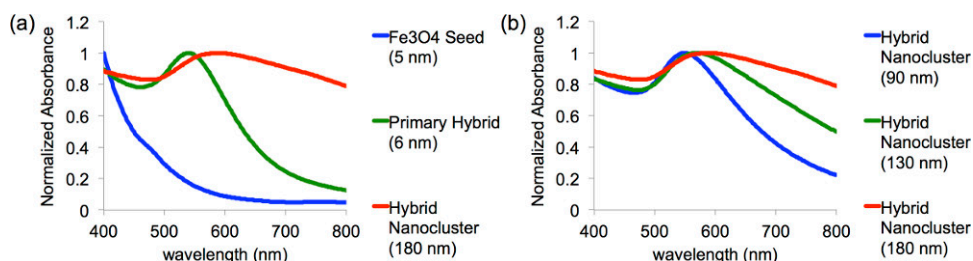


**Figure 4. (A)** UV-Vis-NIR spectra of iron oxide core nanoparticles (blue), gold-coated iron oxide nanoparticles (green), and hybrid magneto-plasmonic nanoclusters (red). **(B)** UV-Vis-NIR spectra of hybrid magneto-plasmonic nanoclusters with various sizes: 90 nm (blue), 130 nm (green), and 180 nm (red). All spectra are normalized to one at the maximum absorbance to show differences in spectral profiles. [Please click here to view a larger version of this figure.](#) [Please click here to view a larger version of this figure.](#)

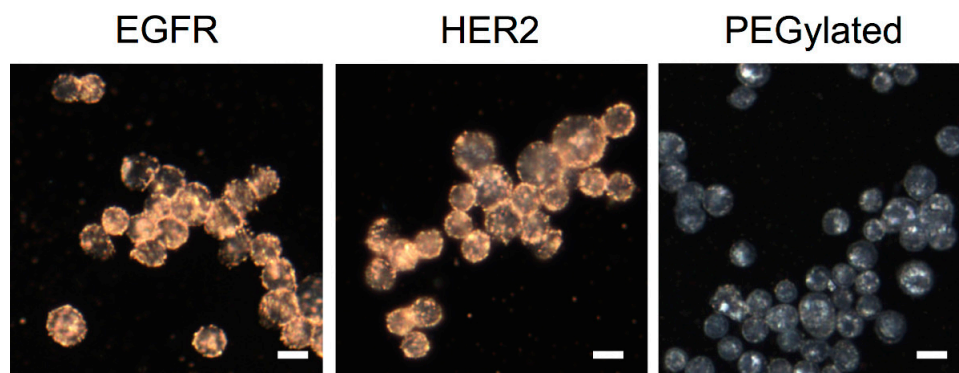


**Figure 5. Molecular specificity of antibody conjugated magneto-plasmonic nanoclusters:** (Left) EGFR expressing A-431 skin cancer cells incubated with EGFR-targeted nanoclusters; (Middle) HER2 expressing SK-BR-3 breast cancer cells incubated with HER2-targeted nanoclusters; (Right) A-431 cells incubated with untargeted PEGylated nanoclusters. The yellow-orange color of cells indicates successful labeling by the functionalized nanoclusters; grey-blue color corresponds to an endogenous scattering from cells. The images were acquired using upright microscope with 20X dark-field objective and Xe lamp excitation. Scale bar is 10  $\mu\text{m}$ . [Please click here to view a larger version of this figure.](#)

**Movie 1.** This video compares a response of A-431 cancer cells labeled by either primary nanoparticles or nanoclusters to an external magnetic field. Both particle types were conjugated with anti-EGFR antibodies for specific targeting of the EGFR(+) A431 cells. First, an Eppendorf tube was filled with a suspension of labeled cells. Then, a magnet was placed next to the tube and motion of cells was imaged at ca. 10 mm away from the magnet. The movie on the left shows cells labeled with primary nanoparticles (6 nm in diameter) and the movie on the right - cells labeled with magneto-plasmonic nanoclusters (100 nm in diameter). The movies were acquired using an inverted microscope in bright-field mode with a 20X objective. Scale bar is 100  $\mu\text{m}$ .

## Discussion

Critical steps in successful synthesis of magneto-plasmonic nanoclusters include making highly monodispersed primary gold shell/iron oxide core nanoparticles and directing self-assembly of the primary particles into nanoclusters. A molar ratio between the primary particles and surfactants play an important role in determining size distribution of the nanoclusters. Non-uniform size distribution of primary nanoparticles may cause formation of big aggregates during assembly of magneto-plasmonic nanoclusters. In addition, the microemulsion method of nanocluster formation relies on amphiphilic surfactants: hydrophobic tail groups hold primary nanoparticles together and hydrophilic head groups stabilize nanoclusters in an aqueous solution. Concentration of surfactants determines nanocluster assembly: a high concentration would lead to formation of smaller nanoclusters or individual primary particles and a low concentration would result in particle aggregation.

As-synthesized nanoclusters have a wide size distribution from ca. 50 nm to ca. 300 nm that requires an additional separation step. Centrifugation with a gradually increasing speed as described in the protocol above produces good results with separated fractions having size distributions  $90 \pm 18$  nm,  $130 \pm 26$  nm, and  $180 \pm 39$  nm. Finer separation to produce narrower distributions should be possible by using a size-exclusion chromatography. It should be also noted that the nanoclusters have a broad absorbance in the red-NIR region that provides an opportunity to excite plasmon resonances with any sources between ca. 500 and 900 nm (**Figure 4**). However, this property also limits applicability of the nanoclusters in simultaneous imaging of multiple targets.

A hydrodynamic radius of nanoclusters increases by  $\sim 10$ -15 nm after antibody conjugation. This increase in diameter correlates well with ca. 12 nm size of an IgG antibody that is attached through the Fc moiety to the surface of nanoparticles. Therefore, the change in the hydrodynamic diameter is consistent with the directional conjugation chemistry of antibodies through the Fc portion that is implemented in the protocol. Zeta potential of nanoparticles shifts from  $-47.6$  mV before antibody conjugation to  $-7.0$  mV after the conjugation. The change of the surface charge provides additional evidence of antibody conjugation to nanoclusters.

The unique feature of the protocol described herein is synthesis of magneto-plasmonic nanoparticles of various sizes from primary blocks which also have magneto-plasmonic characteristics. This method provides a simple way to simultaneously control the strength of plasmonic and magnetic characteristics of the resulting nanostructures. In contrast, previous protocols used an assembly of plasmonic and magnetic nanomaterials where one material served as a template for deposition of the other one; in this approach one material occupies volume and the other surface of the resulting nanostructures. Magneto-plasmonic nanoparticles reported in literature have significantly lower density and the overall amount of superparamagnetic particles as compared to the nanoclusters made by our protocol<sup>14,15</sup>. In our method magnetic and plasmonic moieties are uniformly distributed throughout the volume of hybrid magneto-plasmonic nanoparticles.

## Disclosures

The authors declare that they have no competing financial interests.

## Acknowledgements

This work was supported in part by the NIH grants R01 EB008101 and R01 CA103830.

## References

1. Bigall, N. C., Parak, W. J., & Dorfs, D. Fluorescent, magnetic and plasmonic—Hybrid multifunctional colloidal nano objects. *Nano Today*. **7**, 282-296, doi:10.1016/j.nantod.2012.06.007, (2012).
2. Gautier, J., Allard-Vannier, E., Herve-Aubert, K., Souce, M., & Chourpa, I. Design strategies of hybrid metallic nanoparticles for theragnostic applications. *Nanotechnology*. **24**, 432002, doi:10.1088/0957-4484/24/43/432002, (2013).
3. Wei, Q., & Wei, A. Optical imaging with dynamic contrast agents. *Chemistry*. **17**, 1080-1091, doi:10.1002/chem.201002521, (2011).
4. Aaron, J. S. *et al.* Increased optical contrast in imaging of epidermal growth factor receptor using magnetically actuated hybrid gold/iron oxide nanoparticles. *Optics express*. **14**, 12930-12943, doi:10.1364/OE.14.012930, (2006).
5. Song, H.-M., Wei, Q., Ong, Q. K., & Wei, A. Plasmon-resonant nanoparticles and nanostars with magnetic cores: synthesis and magnetomotive imaging. *ACS nano*. **4**, 5163-5173, doi:10.1021/nn101202h, (2010).
6. Qu, M. *et al.* Magneto-photo-acoustic imaging. *Biomedical optics express*. **2**, 385-396 (2011).
7. Jin, Y., Jia, C., Huang, S.-W., O'Donnell, M., & Gao, X. Multifunctional nanoparticles as coupled contrast agents. *Nature communications*. **1**, 41, doi:10.1038/ncomms1042, (2010).
8. Wu, C.-H. *et al.* Versatile Immunomagnetic Nanocarrier Platform for Capturing Cancer Cells. *ACS nano*. **7**, 8816-8823, doi:10.1021/nn403281e, (2013).
9. Galanzha, E. I. *et al.* *In vivo* magnetic enrichment and multiplex photoacoustic detection of circulating tumour cells. *Nature nanotechnology*. **4**, 855-860, doi:10.1038/nnano.2009.333, (2009).
10. Larson, T. A., Bankson, J., Aaron, J., & Sokolov, K. Hybrid plasmonic magnetic nanoparticles as molecular specific agents for MRI/optical imaging and photothermal therapy of cancer cells. *Nanotechnology*. **18**, 325101, doi:10.1088/0957-4484/18/32/325101, (2007).
11. Yu, H. *et al.* Dumbbell-like bifunctional Au-Fe<sub>3</sub>O<sub>4</sub> nanoparticles. *Nano letters*. **5**, 379-382, doi:10.1021/nl047955q, (2005).
12. Wang, L. *et al.* Monodispersed core-shell Fe<sub>3</sub>O<sub>4</sub>@Au nanoparticles. *The journal of physical chemistry. B*. **109**, 21593-21601, doi:10.1021/jp0543429, (2005).
13. Wang, H., Brandl, D. W., Le, F., Nordlander, P., & Halas, N. J. Nanorice: a hybrid plasmonic nanostructure. *Nano letters*. **6**, 827-832, doi:10.1021/nl060209w, (2006).
14. Hu, X. *et al.* Trapping and Photoacoustic Detection of CTCs at the Single Cell per Milliliter Level with Magneto#Optical Coupled Nanoparticles. *Small*. **9**, 2046-2052, doi:10.1002/smll.201202085, (2013).
15. Truby, R. L., Emelianov, S. Y., & Homan, K. A. Ligand-mediated self-assembly of hybrid plasmonic and superparamagnetic nanostructures. *Langmuir*. **29**, 2465-2470, doi:10.1021/la3037549, (2013).
16. Bai, F. *et al.* A Versatile Bottom#up Assembly Approach to Colloidal Spheres from Nanocrystals. *Angewandte Chemie International Edition*. **46**, 6650-6653, doi:10.1002/ange.200701355, (2007).